

Temperature gradients, and search for non-Boussinesq effects, in the interior of turbulent Rayleigh-Bénard convection

E. BROWN and G. AHLERS

Department of Physics and iQCD, University of California - Santa Barbara, CA 93106, USA

received 6 July 2007; accepted in final form 3 August 2007
published online 28 August 2007

PACS 47.27.-i – Turbulent flows
PACS 47.55.P- – Buoyancy-driven flows; convection

Abstract – We report temperature measurements for a cylindrical sample of turbulent Rayleigh-Bénard convection (RBC) at points in the interior, well away from the thermal boundary layers near the top and bottom of the sample. The aspect ratio was equal to 1.00 and the Prandtl number σ was equal to 4.4 or 5.5. The data are in the range $5 \times 10^7 < R < 10^{10}$, where R is the Rayleigh number. Measurements of the temperatures $T(r, z, \theta)$ at the side wall ($r = L/2$) at eight equally spaced azimuthal positions θ and on three horizontal planes located at vertical positions $z = -L/4, 0, L/4$ (the sample height and diameter are equal to L and $z = 0$ is located at half height) are reported. An analysis of the harmonic contents of $T(L/2, 0, \theta)$ did not reveal any symmetry-breaking deviations from the Oberbeck-Boussinesq approximation even under conditions where the azimuthal average of the center temperature $T_w(z) = \langle T(L/2, z, \theta) \rangle_\theta$ at $z = 0$ differed appreciably from the mean temperature $T_m = (T_t + T_b)/2$ (T_t and T_b are the top and bottom temperatures, respectively). The azimuthal average of the vertical temperature variation $2[T_w(-L/4) - T_w(L/4)]/(T_b - T_t)$ at the side wall, presumably dominated by plume activity, was found to be destabilizing and quite large, ranging from about 0.2 at $R = 5 \times 10^7$ to about 0.06 at $R = 10^{10}$. We also report data for the temperature $T_0(z)$ along the center line ($r = 0$) at $z = -L/4, 0, L/4$. In contrast to $T_w(z)$, $T_0(z)$ revealed a small *stabilizing* gradient $2[T_0(-L/4) - T_0(L/4)]/(T_b - T_t)$ that depended only weakly on R and was about equal to -0.007 for $\sigma = 4.4$ and -0.013 for $\sigma = 5.5$.

Copyright © EPLA, 2007

Introduction. – Turbulence in a fluid heated from below (Rayleigh-Bénard convection [1,2] or RBC) has provided the opportunity to study a number of interesting physical phenomena, [3–5] including the nature of viscous [6,7] and thermal boundary layers, [8–10] the interaction between these layers and a large-scale circulation (LSC) [11–14] in the interior or bulk of the system, interactions between the scale of order the sample height L of the LSC and the small scales of turbulent fluctuations [15–17], and interactions between the LSC and an external field due to rotation provided either by Earth’s Coriolis force [18] or deliberately in the laboratory [19].

In models of this system [12,20–25] it is usually assumed that part of the temperature drop $\Delta T = T_b - T_t$ (T_b and T_t are the temperatures of the bottom and top of the sample) occurs across a thermal boundary layer near the bottom of the sample, and that the remainder of ΔT is found across another such layer near the top. In this approximation the interior, even though fluctuating vigorously, in the time average has a uniform temperature. The purpose

of the present paper is to contribute to our experimental knowledge about the extent of the deviations from these necessary but over-simplified model assumptions.

In this system the temperature difference is usually expressed in terms of the dimensionless combination of parameters [26]

$$R = \frac{\beta g \Delta T L^3}{\kappa \nu} \quad (1)$$

known as the Rayleigh number (here β is the isobaric thermal expansion coefficient, g the acceleration of gravity, κ the thermal diffusivity, and ν the kinematic viscosity). Two further parameters that characterize the system are the Prandtl number $\sigma = \nu/\kappa$ and a measure of the geometrical sample shape. For a cylindrical sample the latter role is played by the aspect ratio $\Gamma \equiv D/L$ (D is the sample diameter). RBC is usually described in terms of the Oberbeck-Boussinesq (OB) approximation, [27,28] where it is assumed that the fluid properties do not vary significantly over the imposed temperature range from

T_t to T_b , except for the density where it provides the buoyancy force. For large enough ΔT this approximation will break down, and interesting deviations from the predictions based on the OB assumption occur [29–32] and are known as non-Oberbeck-Boussinesq (NOB) effects.

For cylinders with $\Gamma = \mathcal{O}(1)$ and R not too large the LSC to a good approximation flows up along the wall and down along the wall at an azimuthal position that differs by π ; *i.e.* the sample contains a single convection roll. Thus, along the top and bottom plates the LSC sweeps across the boundary layers and entrains hot or cold volumes of fluid known as plumes [33] that are emitted by the bottom and top boundary layers, respectively. These plumes in turn add to the LSC by virtue of their excess buoyancy. The LSC/plume combination will cause a temperature increase along the side wall where the fluid is rising, and a decrease on the opposite side where the fluid is falling. The consequent azimuthal variation of the temperature near the side wall and in a horizontal plane has yielded a wealth of information about LSC dynamics and its interaction with the turbulent background fluctuations [15–18,34,35]. Here we will study the influence of the LSC and the plumes that are carried along with it on the time-averaged temperature in the fluid away from the top and bottom boundaries.

One of the objectives of the present paper was to search for NOB effects on the temperature distribution in the interior (or bulk) of the system. One might conjecture that such effects could arise from a difference in the nature of the plumes that are emitted by the two thermal boundary layers. As will be seen below in figs. 2 and 4, the azimuthal variation of the temperature along the side wall and at a given height can be described very well by a cosine of the azimuthal angle θ , with a phase that gives the position of the LSC up-flow. This function and its odd harmonics retain the symmetry between the up-flow and down-flow that is expected for the OB system. Indeed a small contribution, independent of ΔT , from a third harmonic was detected in the measurements. Even harmonics would break the expected OB symmetry. Within our resolution we were unable to detect any contributions from even harmonics. Thus any NOB effects on the LSC-induced temperature profile are small or absent.

The other objective was to gain information about vertical thermal gradients in the bulk of the sample. In many models these are assumed to be absent, but early measurements [36] as well as direct numerical simulations of two-dimensional systems [37,38] showed that this is an approximation. From the azimuthal and time average of the temperatures measured at three vertical positions we found significant destabilizing gradients near the side wall, with temperature drops (extrapolated linearly to the length L of the sample) ranging from 20% of ΔT for R near 10^8 to about 5% of ΔT for R near 10^{10} . On the other hand, along the center line we observed stabilizing temperature differences which were, however only about $\mathcal{O}(1\%)$ of ΔT .

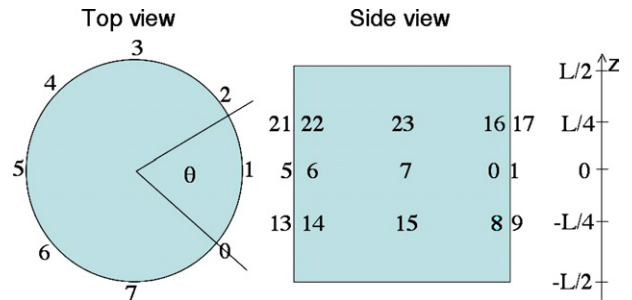


Fig. 1: Schematic diagram of the location of the side-wall thermometers. For the top view only the thermometer locations for the set located a distance $L/2$ above the bottom plate (on the horizontal mid-plane, or $z = 0$) are shown. The side view indicates the location of all three sets.

Their magnitude was found to increase with σ , but they depended only weakly on R .

Apparatus, measurements, and analysis. – The measurements were made using the “medium” sample described in ref. [39]. The sample was a cylinder of height $L = 24.76$ cm and diameter $D = 24.81$ cm, yielding an aspect ratio $\Gamma \equiv D/L = 1.00$. The fluid was water, usually at a mean temperature $T_m = (T_t + T_b)/2 = 40.00$ °C, and unless otherwise stated the results given in this paper are for this temperature. At 40.00 °C $\sigma = 4.38$ and $\nu = 6.7 \times 10^{-7}$ m²/sec. Some measurements were made also at $T_m = 30$ °C where $\sigma = 5.5$. The side wall was made of Plexiglas of thickness 0.31 cm.

We wished to make measurements of the azimuthal temperature variation along the side wall at various vertical positions (such measurements in the top and bottom plate of the sample were made before by Cioni *et al.* [40]). To this end, three sets of eight thermistors each, equally spaced around the circumference at the three vertical positions $z = -L/4, 0$, and $L/4$ (we take the origin of the vertical axis at the horizontal midplane of the sample) and labeled $i = 0, \dots, 7$, etc. as shown in fig. 1, were imbedded in small holes drilled horizontally from the outside into but not penetrating the side wall. The thermistors were able to sense the adjacent fluid temperature without interfering with delicate fluid-flow structures. As discussed in ref. [16], their response time to fluid temperature changes was of the order of a second, which is sufficiently small for the present work. We measured the temperature of each thermistor with a sampling period of about 2.5 seconds. An example for $z = 0$ is shown in fig. 2. Since the LSC carried warm (cold) fluid from the bottom (top) plate up (down) the side wall, these thermistors detected the location of the upflow (downflow) of the LSC by indicating a relatively high (low) temperature.

To determine the orientation and strength of the LSC, we fit the function

$$T(r = L/2, z = 0, \theta) = T_w(z = 0) + \delta_0 \cos\left(\frac{i\pi}{4} - \theta_0\right), \quad (2)$$

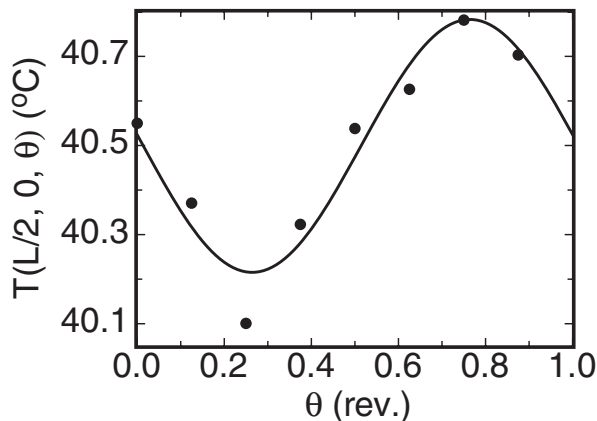


Fig. 2: An example of the temperatures $T(L/2, 0, \theta)$ at the horizontal mid-plane of the side wall as a function of the azimuthal angle θ for $R = 1.1 \times 10^{10}$. Solid line: a fit of eq. (2) to the data. The fit yields the orientation θ_0 and an amplitude $\delta(z=0)$ that reflects the LSC strength.

$i=0, \dots, 7$, separately at each time step, to the eight temperature readings obtained from the thermistors at $z=0$. An example of such a fit is given by the solid line in fig. 2. The measurements scatter about the fitted curve. We attribute this scatter primarily to local fluctuations of the fluid temperature. The fit parameter $\delta_0 = \delta(z=0)$ is a measure of the temperature amplitude of the LSC and θ_0 is the azimuthal orientation of the plane of the LSC circulation. We calculated orientations θ_t and θ_b and amplitudes δ_t and δ_b for the top and bottom levels at $z=L/4$ and $-L/4$, separately, by the same method as for the middle row. Results from this method of determining the orientation and strength of the LSC were reported in several previous publications [15,16,18,34]. Here we focus on the deviations of $T(L/2, z, \theta)$ from the purely harmonic fitting function eq. (2), and on the azimuthal averages $T_w(z)$.

In addition to $T_w(z)$, we measured the temperature $T_0(z)$ along the sample center-line at positions $z = -L/4, 0, L/4$ with three very small thermistors located in the fluid interior.

Amplitude of the azimuthal temperature variation. – For comparison with the size of various other temperature variations to be discussed in the remainder of this paper, it is useful to have at hand the size of the amplitude $\delta(z)$ of the azimuthal temperature variation. Thus, in fig. 3 we show the time-averaged results for δ , normalized by ΔT , as a function of R for all three vertical positions. The amplitude is largest in the middle row at $z=0$.

Search for NOB effects on the azimuthal temperature profile. – In the NOB system at large ΔT , the top and bottom boundary layers differ from each other [31,32]. It is not known whether this asymmetry will lead to an asymmetry of the plumes that are emitted from the

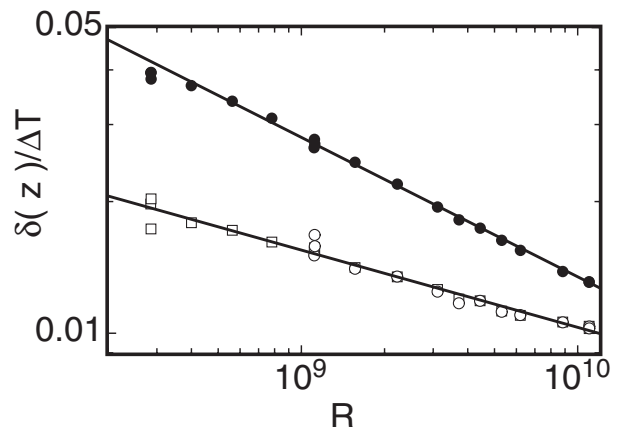


Fig. 3: The LSC temperature amplitude $\delta/\Delta T$ vs. R for the three rows of thermistors. Open squares: $z=L/4$. Solid circles: $z=0$. Open circles: $z=-L/4$. The solid lines are power law fits to the data for $R > 4 \times 10^8$ and correspond to $\delta_0/\Delta T = 21R^{-0.32}$ (upper line) and $\delta_{t,b}/\Delta T = 0.60R^{-0.176}$ (lower line).

boundary layers. A significant difference in the nature of the hot and cold plumes, ascending and descending on opposite sides of the sample, could lead to an asymmetry in the azimuthal temperature profile.

Motivated by this idea, we fitted eq. (2) to each member (consisting of eight temperatures like those in fig. 2) of a data set from a run at constant R , each such run consisting of typically 30000 individual members and spanning typically a time interval of one day. Each fit gave a value of δ_0 and θ_0 , and all results from a given run were used to obtain the normalized time-averaged side-wall temperature-profile $\langle (T - T_w)/\delta_0 \rangle \equiv \langle [T(L/2, 0, \theta) - T_w(0)]/\delta_0 \rangle$ as a function of $\theta - \theta_0$. The process then was repeated at many values of R . An example of $\langle (T - T_w)/\delta_0 \rangle$ is shown in fig. 4. It is for $\Delta T = 20$ K and $R = 1.1 \times 10^{10}$. The solid line is the function $\cos(\theta - \theta_0)$, which should agree with the data if eq. (2) is the correct fitting function. The comparison shows that the fitting function is quite good, but small deviations can be seen in the plot.

The measurements discussed above give the azimuthal variation of the time-averaged temperature immediately at the side wall. Results by Qiu and Tong [13] show that the mean temperature along a diameter connecting the extrema of $\langle (T - T_w)/\delta_0 \rangle$ varies linearly through the sample interior. This implies that $T_w(0) = T_0(0) = T_c$, where T_c is the center temperature defined in ref. [31].

In order to focus on the deviations from the cosine function, we subtracted $\cos(\theta - \theta_0)$ from the temperature profile in fig. 4. The difference is plotted in fig. 5. One sees that the deviations are dominated by a 3rd-harmonic term. The error bars represent the statistical error of the measurements. These deviations represent a very small temperature difference, as they are about 5% of δ_0 , and δ_0 is only 1/80 of ΔT in this case (see fig. 3), so the temperature variation shown here is equivalent to about 12 mK.

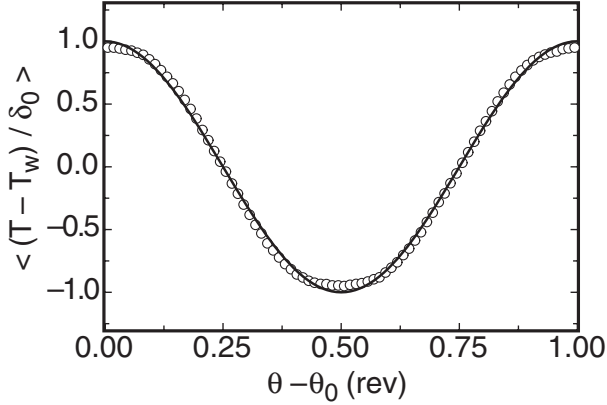


Fig. 4: The normalized time-averaged side-wall temperature-profile $\langle (T - T_w) / \delta_0 \rangle$ for $z = 0$ and as a function of the angle $\theta - \theta_0$. The solid line is the function $\cos(\theta - \theta_0)$, which should agree with the data if the fitting function is chosen well. This example is for $\Delta T = 20$ K and $R = 1.1 \times 10^{10}$.

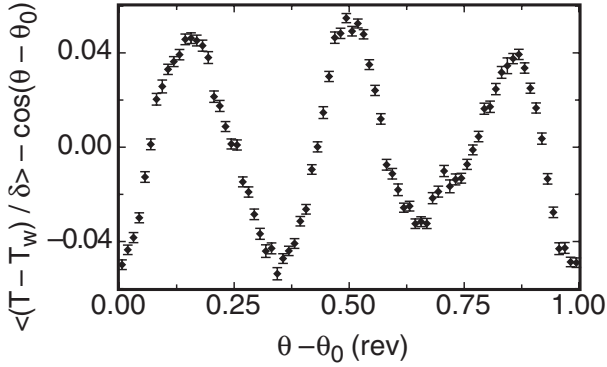


Fig. 5: The average deviations from the cosine fitting profile, given by $\langle (T - T_w) / \delta_0 \rangle - \cos(\theta - \theta_0)$ vs. $\theta - \theta_0$. This is for $\Delta T = 20$ K and $R = 1.1 \times 10^{10}$.

To search for non-Boussinesq effects in the azimuthal temperature profile, we looked for an asymmetry between the up-flow and the down-flow at the horizontal mid-plane by determining the Fourier coefficients of the average temperature profile so that

$$\langle (T - T_w) / \delta_0 \rangle = \sum_n \{a_n \cos[n(\theta - \theta_0)] + b_n \sin[n(\theta - \theta_0)]\}. \quad (3)$$

Since the dominating term is the cosine term with coefficient a_1 , additional terms with $a_n \neq 0$ for odd n keep the temperature profile symmetric, while additional terms with even n would break the symmetry, indicating a non-Boussinesq effect. Terms with $b_n \neq 0$ would indicate an asymmetry of the temperature profile which is not expected to exist even for the NOB system. The first few Fourier coefficients are shown in table 1 for both $\Delta T = 20$ K and $\Delta T = 37$ K. For both ΔT , $a_1 \approx 1$ and $a_3 \approx 0.05$ as we have already seen in figs. 4 and 5. The values of all other coefficients are less than about 0.01, which corresponds to a temperature difference of only a few mK and

Table 1: The first few Fourier coefficients a_n (cosine terms) and b_n (sine terms) obtained by fitting eq. (3) to the side-wall temperature profile.

ΔT	20 K	20 K	37 K	37 K
n	a_n	b_n	a_n	b_n
1	0.9997	-0.0000	0.9997	-0.0001
2	-0.0056	0.0060	-0.0068	-0.0014
3	-0.0512	0.0086	-0.0439	-0.0079
4	-0.0005	-0.0037	-0.0092	-0.0015
5	-0.0011	0.0016	-0.0061	-0.0108

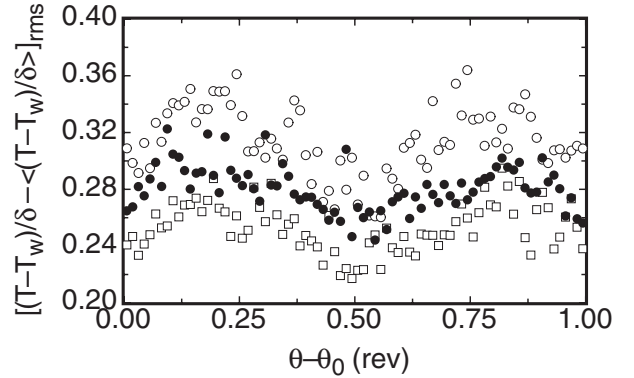


Fig. 6: The temperature fluctuations around the mean profile given by the root-mean-square value of $(T - T_w) / \delta_0 - \langle (T - T_w) / \delta_0 \rangle$ as a function of angle $\theta - \theta_0$. Open circles: $\Delta T = 2.5$ K. Solid circles: $\Delta T = 20$ K. Open squares: $\Delta T = 37$ K. The similarity of the profiles at different ΔT suggests that the fluctuations are not influenced significantly by NOB effects.

is about the resolution of the side-wall thermistors. From this analysis it follows that if there is a NOB effect in the azimuthal temperature profile, it is no larger than about 1% of δ_0 even for $\Delta T = 37^\circ\text{C}$. For comparison, the difference between the center temperature $T_w(z = 0) = T_c$ and the mean temperature T_m in the same experiment was about 2.5% of ΔT (or 500 mK) for $\Delta T = 20$ K, and about 4.3% of ΔT (or 1600 mK) for $\Delta T = 37$ K [31]. Additional details about NOB effects on T_c and on the Nusselt number can be found as well in ref. [31].

The corresponding results for $\langle (T - T_w) / \delta_{t,b} \rangle$ at $z = L/4$ and $-L/4$ were similar to those found for $z = 0$ and will not be shown here.

Fluctuations. – We can also look at the fluctuations around the mean temperature profile. The fluctuations are given by the root-mean-square value of $(T - T_w) / \delta_0 - \langle (T - T_w) / \delta_0 \rangle$ as a function of the angle $\theta - \theta_0$ and are shown in fig. 6 for three different values of ΔT . In a NOB case we might expect the fluctuations to depend on $\theta - \theta_0$, which might indicate a difference in plume activity on the hot ($\theta - \theta_0 = 0$) and cold ($\theta - \theta_0 = 0.5$ rev.) sides of the sample. For each value of ΔT the fluctuations are maximized at intermediate angles, perhaps because both

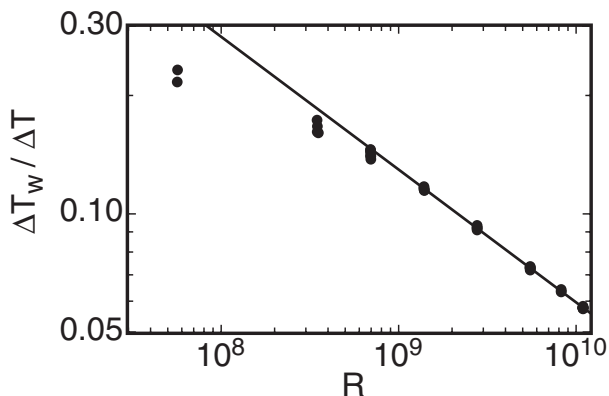


Fig. 7: The non-dimensional bulk temperature difference $\Delta T_{wall}/\Delta T$ measured along the side wall *vs.* R . The solid line is a fit to the data for $R > 10^9$ and corresponds to $\Delta T_w/\Delta T = 141R^{-0.338}$.

hot and cold plumes can appear at these angles, resulting in a larger temperature variation. The profiles appear to be the same for all three values of ΔT , suggesting the absence of significant NOB effect. From a calculation of an analog to a_1 and a_3 for these fluctuations as a measure of the asymmetry, one gets values of a_1 and a_3 that are less than 0.01 for each ΔT . Thus, the difference between the hot and cold sides is again about 1% of δ_0 , which is the limit of our temperature resolution.

Vertical temperature drop. – We measured the average temperatures $T_w(z)$ at the side wall for the three heights $z = -L/4, 0$ and $L/4$. The temperature difference for the bulk is then extrapolated to be $\Delta T_w = 2 \times [T_w(-L/4) - T_w(L/4)]$. This is plotted as a fraction of ΔT in fig. 7. For $R > 10^9$ it can be represented by the power law $141R^{-0.338}$, as shown by the solid line in the figure. One can see that the bulk temperature drop adjacent to the side wall is of the order of 10% of ΔT in our range of R , a surprisingly large value. Indeed it is significantly larger than the horizontal temperature variation $2\delta_0$ at $z = 0$, as can be seen by a comparison with fig. 3. We are not aware of similar measurements by others in the immediate vicinity of the side wall.

Using three thermistors inside the sample, suspended along the central axis on fishing lines at the same 3 heights $z = -L/4, 0$, and $L/4$, the analogous bulk temperature drop $\Delta T_0 = 2 \times [T_0(-L/4) - T_0(L/4)]$ was measured along the central axis for $\sigma = 4.4$ and 5.5 ($\sigma = 5.5$ was achieved by changing the mean temperature of the water to $T_m = 30^\circ\text{C}$). It is shown in fig. 8 as a fraction of ΔT . The temperature gradient on the axis is only weakly dependent on R , but has a significant increase in magnitude with σ . This gradient is much smaller than that along the side wall, and negative. Thus along the central axis the temperature is colder towards the bottom, which is stable to gravity. If the stabilizing gradient is due to the thermal signature of the LSC as it carries heat from the

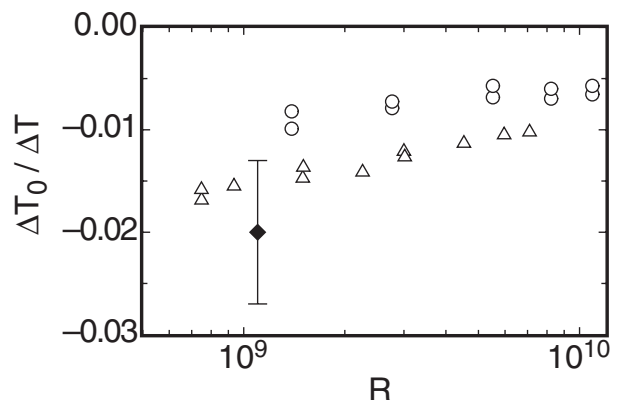


Fig. 8: The non-dimensional bulk temperature drop $\Delta T_0/\Delta T$ measured along the central axis of the cell *vs.* R . Open circles: $\sigma = 4.4$. Open triangles: $\sigma = 5.5$. Solid diamond: from Tilgner *et al.* [36] at $\sigma = 6.6$.

bottom (top) plate to the upper (lower) region of the cell, one expects it to be larger with increasing σ as we found. Because of the small temperature differences measured, the thermistors were re-calibrated after taking data at each R and some measurements were repeated. The pairs of points at the same R seen in fig. 8 show that the measurements are repeatable to within about 1 mK in ΔT_0 .

Measurements near the sample center have been made by several previous investigators. Du and Tong [9], using water at 30°C ($\sigma = 5.4$), within their resolution found a uniform temperature away from the thermal boundary layers. On the other hand, in good agreement with our result, Tilgner *et al.* [36] using water at 22°C ($\sigma = 6.6$) found that the interior of their sample was stably stratified. Their value of $\Delta T_0/\Delta T \simeq -0.020 \pm 0.007$ is within its quoted uncertainty consistent with our own data. We note that Tilgner *et al.* used a cubic cell whereas ours is cylindrical; it is not known how much the geometry could influence the result.

Stabilizing gradients along the axis have been found also in direct numerical simulations (DNS) of the Boussinesq equations [37,38]. However, a comparison with the present experiment can only be qualitative because these DNS were for aspect ratio 2 of a sample with a square cross section, used free-slip boundary conditions for the velocity at the side wall, and were for $R = 10^6$ which is well below our range of R . Further, the laterally averaged vertical temperature profile was reported and may differ from the measured profile along the center line. Nonetheless, it is interesting to see that the numerical results yielded virtually no gradient for $\sigma = 1$ and a significantly stabilizing gradient for $\sigma = 100$.

Summary. – In many models of turbulent RBC it is assumed that the interior of the sample, although fluctuating vigorously, has a time-averaged temperature that is spatially uniform. It is of interest to determine deviations

from this simplifying assumption. We presented experimental measurements of temperatures in the interior of a turbulent Rayleigh-Bénard sample under conditions where the usual NOB effects caused deviations of the sample center temperature T_c from the mean temperature T_m of up to 1.6 °C or 4% of the applied temperature difference ΔT . Data for the temperature $T(L/2, z, \theta)$ along the side wall at $r = L/2$ of the cylindrical sample at three different heights z showed that the azimuthal variation of this temperature could be represented quite well by a cosine function with an amplitude of a few % of ΔT . The higher-harmonic contents of this azimuthal variation was examined and revealed no asymmetries between the up-flow and the down-flow of the LSC, suggesting that any differences between the plumes that emerge from the top and bottom boundary layers do not have a significant influence on this temperature distribution.

The azimuthal average $T_w(z)$ at the side wall revealed a destabilizing temperature variation that varied with Rayleigh number R from about 20% to about 6% of ΔT as R changed from 10^8 to 10^{10} . In contrast to this, the center temperature $T_0(z)$ showed a *stabilizing* variation which however had a much smaller magnitude that was $\mathcal{O}(1\%)$ of ΔT and increased with σ .

We appreciate the difficulties of developing models for this complex system, but suggest that for some purposes some of the temperature variations reported here will have to be taken into consideration. An example is the modeling of the LSC [35] where the azimuthal temperature variation provides the driving force.

The authors are grateful to S. GROSSMANN and D. LOHSE for fruitful discussions. This work was supported by Grant DMR07-02111 of the US National Science Foundation.

REFERENCES

- [1] BÉNARD H., *Rev. Gen. Sci. Pure Appl.*, **11** (1900) 1261; 1309.
- [2] BÉNARD H., *Ann. Chim. Phys.*, **23** (1901) 62.
- [3] SIGGIA E., *Annu. Rev. Fluid Mech.*, **26** (1994) 137.
- [4] KADANOFF L., *Phys. Today*, **54**, No. 8 (2001) 34.
- [5] AHLERS G., GROSSMANN S. and LOHSE D., *Phys. J.*, **1** (2002) 31.
- [6] QIU X.-L. and XIA K.-Q., *Phys. Rev. E*, **58** (1998) 486.
- [7] QIU X.-L. and XIA K.-Q., *Phys. Rev. E*, **58** (1998) 5816.
- [8] LUI S.-L. and XIA K.-Q., *Phys. Rev. E*, **57** (1998) 5494.
- [9] DU Y.-B. and TONG P., *J. Fluid Mech.*, **407** (2000) 57.
- [10] WANG J. and XIA K.-Q., *Eur. Phys. J. B*, **32** (2003) 127.
- [11] KRISHNAMURTY R. and HOWARD L. N., *Proc. Natl. Acad. Sci. U.S.A.*, **78** (1981) 1981.
- [12] CASTAING B., GUNARATNE G., HESLOT F., KADANOFF L., LIBCHABER A., THOMAE S., WU X.-Z., ZALESKI S. and ZANETTI J., *J. Fluid Mech.*, **204** (1989) 1.
- [13] QIU X.-L. and TONG P., *Phys. Rev. E*, **64** (2001) 036304.
- [14] SUN C., XIA K.-Q. and TONG P., *Phys. Rev. E*, **72** (2005) 026302.
- [15] BROWN E., NIKOLAENKO A. and AHLERS G., *Phys. Rev. Lett.*, **95** (2005) 084503.
- [16] BROWN E. and AHLERS G., *J. Fluid Mech.*, **568** (2006) 351.
- [17] FUNFSCHILLING D., BROWN E. and AHLERS G., submitted to *J. Fluid Mech.* (2007).
- [18] BROWN E. and AHLERS G., *Phys. Fluids*, **18** (2006) 125108.
- [19] HART J. E., KITTELMAN S. and OHLSEN D. R., *Phys. Fluids*, **14** (2002) 955.
- [20] MALKUS W. V. R., *Proc. R. Soc. London, Ser. A*, **225** (1954) 196.
- [21] PRIESTLEY C. H. B., *Q. J. R. Meteorol. Soc.*, **85** (1959) 415.
- [22] SHRAIMAN B. I. and SIGGIA E., *Phys. Rev. A*, **42** (1990) 3650.
- [23] GROSSMANN S. and LOHSE D., *J. Fluid Mech.*, **407** (2000) 27.
- [24] GROSSMANN S. and LOHSE D., *Phys. Rev. Lett.*, **86** (2001) 3316.
- [25] GROSSMANN S. and LOHSE D., *Phys. Rev. E*, **66** (2002) 016305.
- [26] RAYLEIGH LORD, *Philos. Mag.*, **32** (1916) 529.
- [27] OBERBECK A., *Ann. Phys. Chem.*, **7** (1879) 271.
- [28] BOUSSINESQ J., *Théorie analytique de la chaleur*, Vol. 2 (Gauthier-Villars, Paris) 1903.
- [29] WU X.-Z. and LIBCHAER A., *Phys. Rev. A*, **43** (1991) 2833.
- [30] ZHANG J., CHILDRESS S. and LIBCHAER A., *Phys. Fluids*, **9** (1997) 1034.
- [31] AHLERS G., BROWN E., FONTENELE ARAUJO F., FUNFSCHILLING D., GROSSMANN S. and LOHSE D., *J. Fluid Mech.*, **569** (2006) 409.
- [32] AHLERS G., FONTENELE ARAUJO F., FUNFSCHILLING D., GROSSMANN S. and LOHSE D., *Phys. Rev. Lett.*, **98** (2007) 054501.
- [33] XI H.-D., LAM S. and XIA K.-Q., *J. Fluid Mech.*, **503** (2004) 47.
- [34] AHLERS G., BROWN E. and NIKOLAENKO A., *J. Fluid Mech.*, **569** (2005) 409.
- [35] BROWN E. and AHLERS G., *Phys. Rev. Lett.*, **98** (2007) 134501.
- [36] TILGNER A., BELMONTE A. and LIBCHAER A., *Phys. Rev. E*, **47** (1993) R2253.
- [37] SCHMALZL J., BREUER M. and HANSEN U., *Geophys. Astrophys. Fluid Dyn.*, **96** (2002) 381.
- [38] BREUER M., WESSLING S., SCHMALZL J. and HANSEN U., *Phys. Rev. E*, **69** (2004) 026302.
- [39] BROWN E., NIKOLAENKO A., FUNFSCHILLING D. and AHLERS G., *Phys. Fluids*, **17** (2005) 075108.
- [40] CIONI S., CILIBERTO S. and SOMMERIA J., *J. Fluid Mech.*, **335** (1997) 111.